All strongly-cyclic branched coverings of $(1,1)$-knots are Dunwoody manifolds

Alessia Cattabriga   Michele Mulazzani

Abstract

We show that every strongly-cyclic branched covering of a $(1,1)$-knot is a Dunwoody manifold. This result, together with the converse statement previously obtained by Grasselli and Mulazzani, proves that the class of Dunwoody manifolds coincides with the class of strongly-cyclic branched coverings of $(1,1)$-knots. As a consequence, we obtain a parametrization of $(1,1)$-knots by 4-tuples of integers. Moreover, using a representation of $(1,1)$-knots by the mapping class group of the twice punctured torus, we provide an algorithm which gives the parametrization of all torus knots in $\mathbf{S}^3$.

Mathematics Subject Classification 2000: Primary 57M12, 57N10; Secondary 57M25.
Keywords: $(1,1)$-knots, cyclic branched coverings, Heegaard diagrams, Dunwoody manifolds, torus knots, cyclically presented groups.

1 Introduction

In order to investigate the relations between cyclic branched coverings of knots in $\mathbf{S}^3$ and manifolds admitting cyclically presented fundamental groups, M. J. Dunwoody introduced in [6] a class of 3-manifolds depending on six integer parameters. As proved in [7], all these manifolds turn out to be strongly-cyclic coverings of lens spaces (possibly $\mathbf{S}^3$), branched over $(1,1)$-knots. Moreover, it has been shown in [10] that every n-fold strongly-cyclic branched covering of a $(1,1)$-knot admits a genus n Heegaard diagram encoding a cyclic presentation for the fundamental group. This result has been improved in [3], obtaining a constructive algorithm which, starting from

a representation of $(1,1)$-knots through the elements of the mapping class group of the twice punctured torus, explicitly gives the cyclic presentations.

In this paper we prove that all strongly-cyclic branched coverings of $(1,1)$-knots are actually Dunwoody manifolds. As a consequence, the class of Dunwoody manifolds coincides with the class of strongly-cyclic branched coverings of $(1,1)$-knots.

We also obtain, as a further consequence, a parametrization of all $(1,1)$-knots (with the exception of the "core" knot $\{P\} \times \mathbf{S}^1 \subset \mathbf{S}^2 \times \mathbf{S}^1$, which admits no strongly-cyclic branched coverings) by means of four of the six Dunwoody parameters. Moreover, we give an algorithm that allows us to find the parametrization of all torus knots in $\mathbf{S}^3$.

We refer to [9, 2] for details on knot theory and cyclic branched coverings of knots, and to [8] for details on cyclic presentations of groups.

2 Strongly-cyclic branched coverings of (1,1)-knots and Dunwoody manifolds

An n-fold cyclic covering of a 3-manifold N^3 branched over a knot $K \subset N^3$ is called *strongly-cyclic* if the branching index of K is n (i.e., the fiber of each point of K contains a single point). So the homology class of a meridian loop m around K is mapped by the associated monodromy $\omega : H_1(N^3 - K) \to \mathbb{Z}_n$ to a generator of $\mathbb{Z}_n$ (up to equivalence we can always suppose $\omega[m] = 1$).

Observe that a cyclic branched covering of a knot K in $\mathbf{S}^3$ is always strongly-cyclic and uniquely determined, up to equivalence, since $H_1(\mathbf{S}^3 - K) \cong \mathbb{Z}$. Obviously, this property is no longer true for a knot in a more general 3-manifold. Also, if p is a prime number, any p-fold cyclic branched covering of a knot K is automatically strongly-cyclic.

In this paper we deal with strongly-cyclic branched coverings of $(1,1)$-knots, which are knots in lens spaces (possibly in $\mathbf{S}^3$).

A knot K in a 3-manifold N^3 is called a $(1,1)$-*knot* if there exists a Heegaard splitting of genus one

$$(N^3, K) = (H, A) \cup_\varphi (H', A'),$$

where H and H' are solid tori, $A \subset H$ and $A' \subset H'$ are properly embedded trivial arcs, and $\varphi : (\partial H', \partial A') \to (\partial H, \partial A)$ is an attaching homeomorphism (see Figure 1). Obviously, N^3 turns out to be a lens space $L(p,q)$ (including $\mathbf{S}^3 = L(1,0)$).

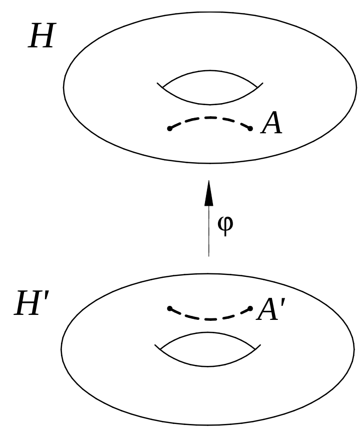

Figure 1: A $(1,1)$-decomposition.

It is well known that the family of $(1,1)$-knots contains all torus knots and all two-bridge knots in $\mathbf{S}^3$. Several topological properties of $(1,1)$-knots have recently been investigated (see references in [4]).

Proposition 1. *A $(1,1)$-knot $K \subset L(p,q)$ with $(1,1)$-decomposition $(L(p,q),K) = (H,A) \cup_\varphi (H',A')$ is completely determined, up to equivalence, by $\varphi(\beta')$, where β' is the boundary of a meridian disk $D' \subset H'$ which does not intersect A'. Moreover, if $(L(p,q),\bar{K}) = (H,A) \cup_{\bar{\varphi}} (H',A')$ is a decomposition of a $(1,1)$-knot $\bar{K}$ such that $\bar{\varphi}(\beta')$ is isotopic to $\varphi(\beta')$ in $\partial H - \partial A$, then $\bar{K}$ is equivalent to K.*

Proof. The first statement follows from the fact that two properly embedded trivial arcs in a ball B, with the same endpoints, are isotopic rel ∂B. The second statement is straightforward. $\square$

An algebraic representation of $(1,1)$-knots has been developed in [3] and [4], where it is shown that there is a natural surjective map

$$\psi \in PMCG_2(\partial H) \mapsto K_\psi \in \mathcal{K}_{1,1}$$

from the pure mapping class group of the twice punctured torus $PMCG_2(\partial H)$ to the class $\mathcal{K}_{1,1}$ of all $(1,1)$-knots. Using this representation, the necessary and sufficient conditions for the existence and uniqueness of an n-fold strongly-cyclic branched covering of a $(1,1)$-knot have been obtained (see [3]).

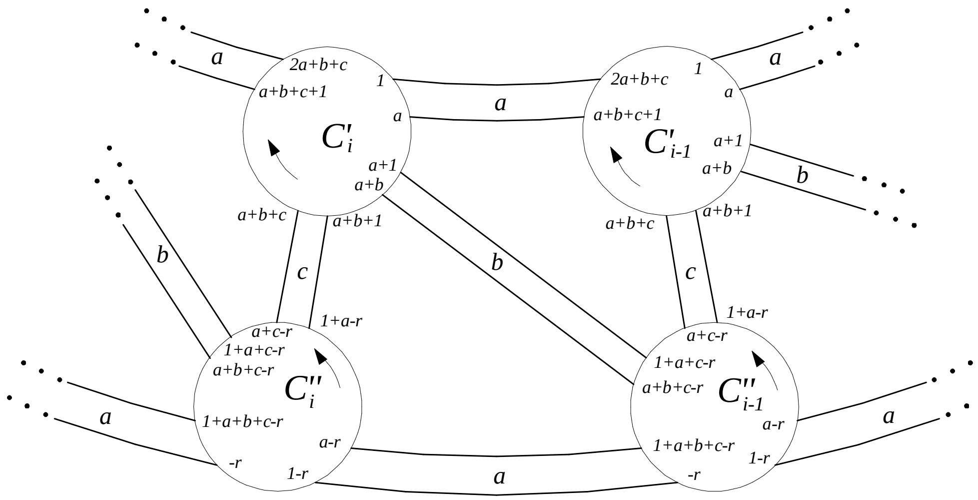

Figure 2: The diagram $D(a, b, c, n, r, s)$, for $a + b + c > 0$.

The family of Dunwoody manifolds has been introduced in [6] by a class of trivalent regular planar graphs (called *Dunwoody diagrams*), depending on six integers a, b, c, n, r, s, such that $n > 0$, $a, b, c \geq 0$. For certain values of the parameters, called *admissible*, the Dunwoody diagrams $D(a, b, c, n, r, s)$ turn out to be Heegaard diagrams, hence defining a wide class of closed, orientable 3-manifolds $M(a, b, c, n, r, s)$ with cyclically presented fundamental groups, called *Dunwoody manifolds*.

More precisely, an admissible Dunwoody diagram $D(a, b, c, n, r, s)$ is an open Heegaard diagram of genus n, with cyclic symmetry of order n. It contains n internal circles $C'_1, \ldots, C'_n$, and n external circles $C''_1, \ldots, C''_n$, each having $d = 2a + b + c$ vertices. These circles represent the first system of curves of the Heegaard splitting. If $d > 0$, as shown in Figure 2, the circle C'_i (resp. C''_i) is connected to the circle C'_{i+1} (resp. C''_{i+1}) by a parallel arcs, to the circle C''_i by c parallel arcs and to the circle C''_{i-1} by b parallel arcs, for every $i = 1, \ldots, n$ (subscripts mod n). If $d = 0$ (i.e., $a = b = c = 0$), there are no arcs connecting the circles, and the diagram (called *trivial*) contains other n circles $C_1, \ldots, C_n$, as depicted in Figure 3.

We denote by $\mathcal{E}$ the set of arcs when $d > 0$, or the set of curves $C_1, \ldots, C_n$ when $d = 0$. Obviously, $\mathcal{E}$ represents the second system of curves of the Heegaard splitting. To reconstruct the splitting, the circle C'_i must be glued to the circle C''_{i+s}, so that, when $d > 0$, equally labelled vertices are identified

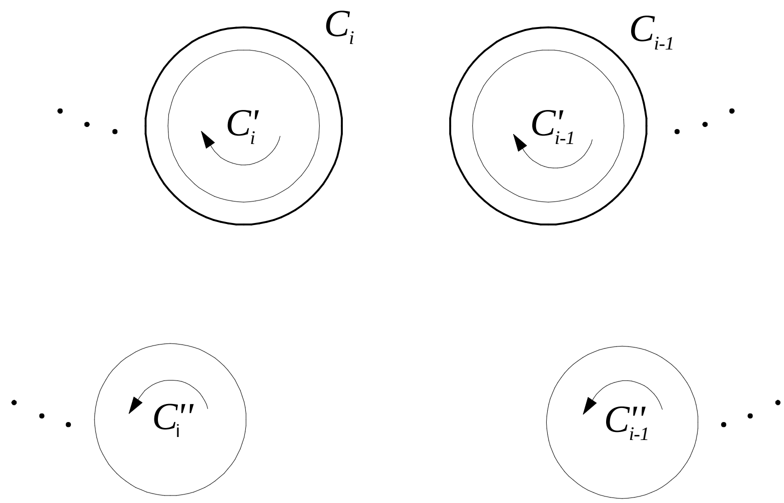

Figure 3: The diagram $D(0, 0, 0, n, r, s)$.

together. Observe that the parameters r and s can be considered mod d and n respectively, and we can suppose $r = 0$ when $d = 0$. Since the identification rule and the diagram are invariant with respect to an obvious cyclic action of order n, the Dunwoody manifold $M(a, b, c, r, n, s)$ admits a cyclic symmetry of order n. Of course, $M(a, b, c, 1, r, 0)$ is homeomorphic to a lens space or to $\mathbf{S}^3$, since it admits a genus one Heegaard splitting. Moreover, the trivial case $M(0, 0, 0, n, 0, s)$ is homeomorphic to the connected sum of n copies of $\mathbf{S}^2 \times \mathbf{S}^1$, for all n and s.

A characterization of all Dunwoody manifolds as strongly-cyclic branched coverings of $(1, 1)$-knots is given by the following result.

Proposition 2. [7] *The Dunwoody manifold $M(a, b, c, n, r, s)$ is the n-fold strongly-cyclic covering of the lens space $M(a, b, c, 1, r, 0)$ (possibly $\mathbf{S}^3$), branched over a $(1, 1)$-knot only depending on the integers a, b, c, r.*

An interesting example of a Dunwoody manifold is $M(1, 1, 1, 3, 2, 1)$, which is homeomorphic to $\mathbf{S}^1 \times \mathbf{S}^1 \times \mathbf{S}^1$. It is well known that this manifold cannot be a cyclic branched covering of any knot in $\mathbf{S}^3$, but turns out to be a 3-fold cyclic covering of $\mathbf{S}^2 \times \mathbf{S}^1 \cong M(1, 1, 1, 1, 2, 0)$, branched over a $(1, 1)$-knot, which will be referred to as $K(1, 1, 1, 2)$.

In the next section we prove the converse of Proposition 2. As a consequence, the class of Dunwoody manifolds coincides with the class of strongly-

cyclic branched coverings of $(1,1)$-knots.

3 Main result

Now we establish the main result of this paper.

Theorem 3. *Every strongly-cyclic branched covering of a* $(1,1)$*-knot is a Dunwoody manifold.*

Proof. Let $K \subset L(p,q)$ be a $(1,1)$-knot and let $(L(p,q),K) = (H,A) \cup_\varphi (H',A')$ be a $(1,1)$-decomposition of K. Let β (resp. β') be a meridian of ∂H (resp. $\partial H'$) that bounds a disc in H (resp. H') not intersecting A (resp. A'). The system of curves $(\beta, \varphi(\beta'))$ on $T = \partial H$ defines a genus one Heegaard diagram of $L(p,q)$, which does not intersect $\partial A = \{N,S\}$. Let H_φ be the open Heegaard diagram on $\mathbb{R}^2$ obtained by cutting T along β, and considering S as the point at the infinity of $\mathbf{S}^2 = \mathbb{R}^2 \cup \{S\}$. The diagram consists of two canonical circles C' and C'', corresponding to β, and a closed curve or a set of arcs with endpoints on the canonical circles, which corresponds to $\varphi(\beta')$ and will be denoted by $\mathcal{E}$. Suppose that one of the following holds:

(1) H_φ is the diagram depicted in Figure 4 a);

(2) H_φ is the diagram depicted in Figure 4 b);

(3) there exist integers a,b,c, with $a,b,c \geq 0$ and $a+b+c > 0$, such that H_φ is the diagram depicted in Figure 5.

In the first case, K is the core knot $\{P\} \times \mathbf{S}^1 \subset \mathbf{S}^2 \times \mathbf{S}^1$, where P is a point of $\mathbf{S}^2$. Therefore, from [3, Cor. 2], we have $H_1(\mathbf{S}^2 \times \mathbf{S}^1 - K) = \langle \alpha, \gamma \,|\, \gamma \rangle \cong \mathbb{Z}$, where α and γ are the curves on T depicted in Figure 6. So, by [3, Th. 4], there exists no strongly-cyclic branched covering of K.

In the second case, K is the trivial knot in $\mathbf{S}^2 \times \mathbf{S}^1$. Therefore, by [3, Cor. 2], we have $H_1(\mathbf{S}^2 \times \mathbf{S}^1 - K) = \langle \alpha, \gamma \,|\, \emptyset \rangle \cong \mathbb{Z} \oplus \mathbb{Z}$. So, by [3, Th. 4], there exist exactly n n-fold strongly-cyclic branched coverings of K, depending on the choice of $\omega(\alpha) \in \mathbb{Z}_n$, where $\omega : H_1(\mathbf{S}^2 \times \mathbf{S}^1 - K) \to \mathbb{Z}_n$ is the monodromy map of the covering such that $\omega(\gamma) = 1$. If we denote by $C_{n,s}(K)$ the n-fold strongly-cyclic branched covering of K such that $\omega(\alpha) = s$, we have $C_{n,s}(K) = M(0,0,0,n,0,s)$. Actually, as previously observed, $C_{n,s}(K)$ is homeomorphic to the connected sum of n copies of $\mathbf{S}^2 \times \mathbf{S}^1$, for all n,s.

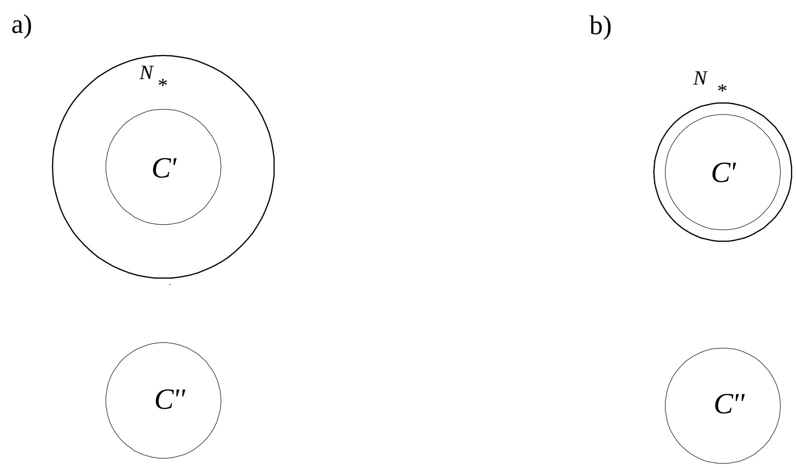

Figure 4:

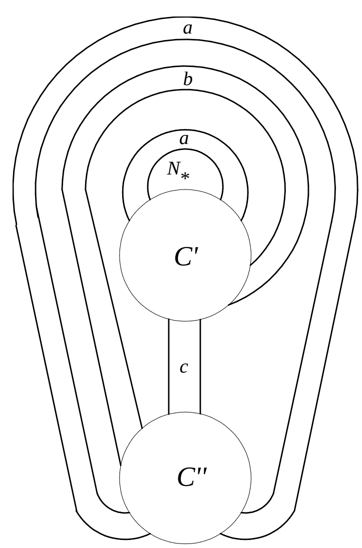

Figure 5:

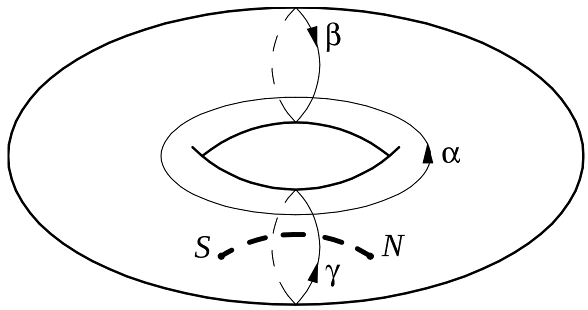

Figure 6:

Let us consider the third case. If $f : M \to L(p,q)$ is an n-fold strongly-cyclic branched covering of K, then the $(1,1)$-decomposition of K lifts to a genus n Heegaard splitting for M (see [10]). Since $\omega(\gamma) = 1$, up to equivalence, then the lifting of H_φ is the Dunwoody diagram $D(a,b,c,n,r,s)$, where $s = \omega(\alpha)$. In other words, M is the Dunwoody manifold $M(a,b,c,n,r,s)$.

By Proposition 1, to prove the theorem it is enough to show that H_φ is equivalent, up to Singer moves fixing N, to one of the three diagrams discussed above.

Denote by D' and D'' the disks of $\mathbb{R}^2$ bounded by C' and C'', respectively. Moreover, let $\mathcal{A}'$ (resp. $\mathcal{A}''$) be the set of arcs of $\mathcal{E}$ with both the endpoints on C' (resp. C''), and denote by $\mathcal{B}$ the remaining arcs of $\mathcal{E}$. Of course, $|\mathcal{A}'| = |\mathcal{A}''|$. An arc $e \in \mathcal{A}'$ (resp. $\mathcal{A}''$) is called *trivial* if the closed curve $e \cup e'$, where e' is one of the two arcs of C' (resp. C'') with the same endpoints of e, bounds a disc containing neither N nor D'' (resp. D'). As illustrated in Figure 7, each trivial arc can be removed by a Singer move of type IB (see [11]). So, up to equivalence, we can suppose that H_φ contains no trivial arcs. Observe that this assumption implies that $e \cup e'$ bounds a disc in $\mathbb{R}^2$ containing the point N, for every $e \in \mathcal{A}' \cup \mathcal{A}''$. In fact, if there exists a non trivial arc e of $\mathcal{A}'$ (resp. of $\mathcal{A}''$) such that $e \cup e'$ bounds a disk D in $\mathbb{R}^2$ not containing N, then D contains D'' (resp. D') and therefore there exists a trivial arc in $\mathcal{A}''$ (resp. $\mathcal{A}'$).

In order to simplify the proof, let us consider the planar graph Γ obtained from H_φ by collapsing the disks D' and D'' to their centers, that we still indicate by C' and C'', respectively. Of course, the arcs of $\mathcal{A}'$ and $\mathcal{A}''$ become loops in Γ bounding disks all containing N.

We say that two elements of $\mathcal{E}$ are *parallel* if they are isotopic rel

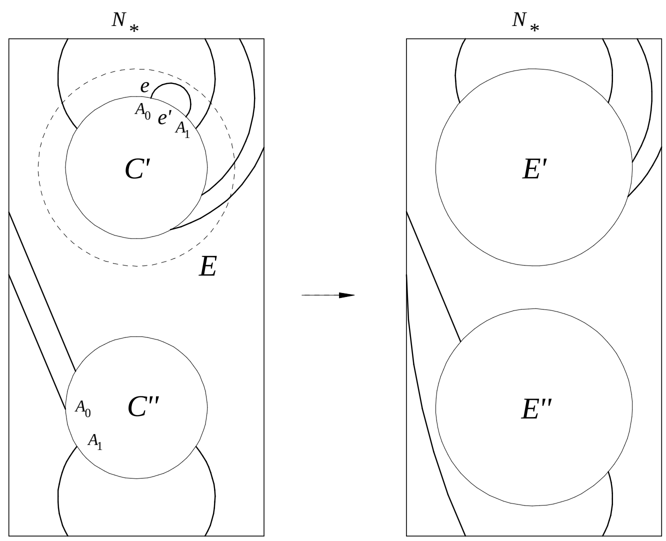

Figure 7: Singer move of type IB.

$\{C', C'', N\}$. It is easy to see that any two elements of $\mathcal{A}'$ (resp. of $\mathcal{A}''$) are parallel. In fact, if the disk bounded by a loop of $\mathcal{A}'$ (resp. $\mathcal{A}''$) contains C'' (resp. C'), then all the disks bounded by the loops of $\mathcal{A}'$ (resp. $\mathcal{A}''$) contain C'' (resp. C'). Otherwise, each loop of $\mathcal{A}''$ (resp. $\mathcal{A}'$) bounds a disk not containing N. As regards the elements of $\mathcal{B}$, we note that two different arcs $g, g' \in \mathcal{B}$ are parallel if and only if the closed curve $g \cup g'$ bounds a disc $D_{g,g'}$ not containing N. It is not difficult to see that there are at most two isotopy classes. For, if $g, g', g'' \in \mathcal{B}$ are different arcs such that g is not parallel to either g' or g'', then $N \in D_{g,g'}$ and $N \in D_{g,g''}$. Moreover, either $D_{g',g''} = (D_{g,g'} - D_{g,g''}) \cup g''$ or $D_{g',g''} = (D_{g,g''} - D_{g,g'}) \cup g'$. In both cases $N \notin D_{g',g''}$ and therefore g' is parallel to g''.

If $\mathcal{A}' = \mathcal{A}'' = \mathcal{B} = \emptyset$, $\mathcal{E}$ consists of a closed curve C. So, up to isotopy in $\mathbb{R}^2 - N$, we can suppose that C is a standard circle. There are two possibilities, depending on whether the point N is contained inside or outside C. But, in both cases, since C is a curve of a Heegaard diagram, C' is inside C if and only if C'' is outside C. So, up to a possible exchange between C' and C'', the two possibilities are those depicted in Figure 8, which are the same as in Figure 4.

If $\mathcal{A}' \cup \mathcal{A}'' \cup \mathcal{B} \neq \emptyset$, we can consider the graph Γ' obtained from Γ by taking only one element for each isotopy class of arcs. So Γ' is a graph embedded

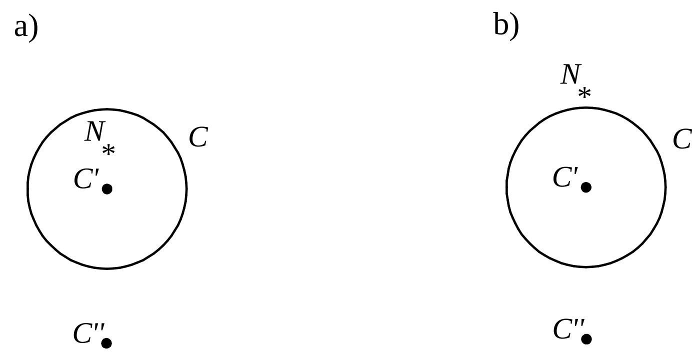

Figure 8:

in $\mathbb{R}^2 - N$ with two vertices, a loop in each vertex if $\mathcal{A}' \neq \emptyset$, and one or two edges linking the vertices if $\mathcal{B} \neq \emptyset$. If $\mathcal{A}' \neq \emptyset$, one of the two loops is contained in the disk bounded by the other, since both of the disks bounded by the loops contain N. Up to isotopy in $\mathbb{R}^2 - N$ and to a possible exchange between C' and C'', they are as in Figure 9. The other edges of Γ', if any, must be contained in the annulus bounded by the two loops. So, up to an isotopy of $\mathbb{R}^2 - N$, which can be chosen as the identity outside C'', they are as in Figure 10. Of course, the same configuration of these edges holds when $\mathcal{A}' = \emptyset$.

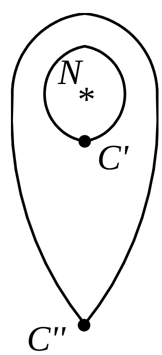

Figure 9:

So H_φ is the diagram depicted in Figure 5, where a, b, c are the cardinalities of the isotopy classes. $\square$

By Theorem 3 and Proposition 2 we have:

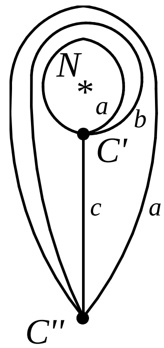

Figure 10:

Corollary 4. *The class of Dunwoody manifolds coincides with the class of strongly-cyclic branched coverings of* $(1,1)$*-knots.*

4 $(\mathbf{1},\mathbf{1})$-knots parametrization

As a consequence of the proof of Theorem 3, any $(1,1)$-knot K, with the sole exception of the core knot $\{P\}\times\mathbf{S}^1 \subset \mathbf{S}^2\times\mathbf{S}^1$ (which admits no strongly-cyclic branched coverings), has a $(1,1)$-decomposition which can be represented by an admissible Dunwoody diagram $D(a,b,c,1,r,0)$, for suitable integers $a,b,c \geq 0$ and r. In this case, we set $K = K(a,b,c,r)$, and we have that the Dunwoody manifold $M(a,b,c,n,r,s)$ is an n-fold strongly-cyclic branched covering of the lens space $M(a,b,c,1,r,0)$ (possibly homeomorphic to $\mathbf{S}^3$), branched over the $(1,1)$-knot $K(a,b,c,r)$.

Examples. By [7, Theorem 8], the two-bridge knot with Schubert parametrization $(2a+1,2r)$ is the $(1,1)$-knot $K(a,0,1,r)$. The trivial knot in $\mathbf{S}^2\times\mathbf{S}^1$ is $K(0,0,0,0)$ and the trivial knot in $L(p,q)$ (including $L(1,0)\cong\mathbf{S}^3$) is $K(0,0,p,q)$.

Note that a different parametrization of $(1,1)$-knots, which involves four parameters for the knot and two additional parameters for the ambient space, can be found in [5].

Now we describe an algorithm that gives the parametrization $K(a,b,c,r)$ of all torus knots in $\mathbf{S}^3$.

Given a closed simple curve $\delta \in \partial H$, denote by $t_\delta \in PMCG_2(\partial H)$ the

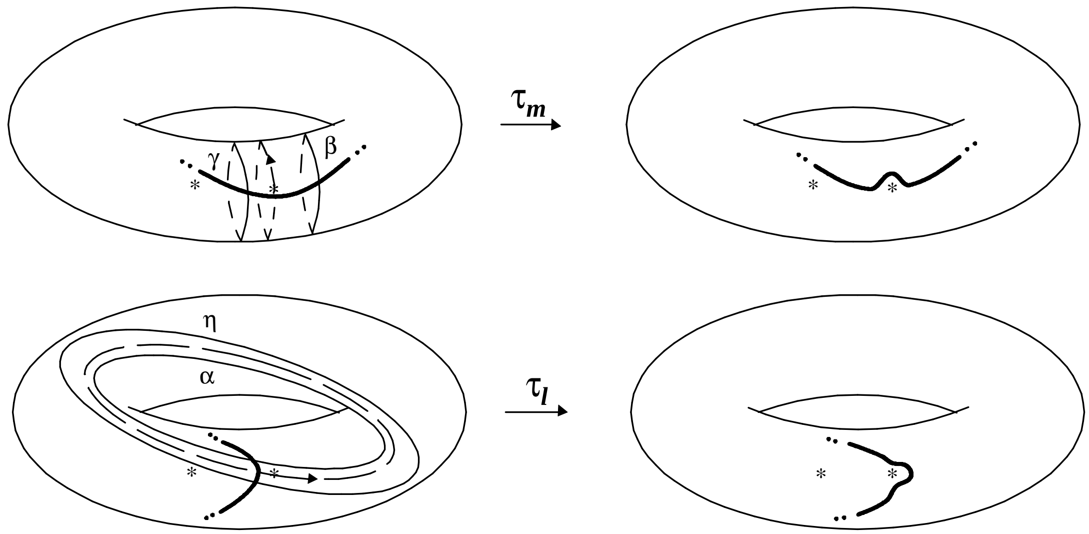

Figure 11: Action of τ_m and τ_l.

right-hand Dehn twist along δ. Moreover, let $\tau_m = t_\beta t_\gamma^{-1}$ and $\tau_l = t_\eta t_\alpha^{-1}$, where $\beta, \gamma, \alpha, \eta$ are the curves depicted in Figure 11. The effect of τ_m and τ_l is to slide one puncture, for example N, along the dashed curves depicted in Figure 11, i.e. along a meridian and a longitude of the torus, respectively.

As shown in [4], for every $1 < k < h$, the torus knot $\mathbf{t}(k,h) \subset \mathbf{S}^3$ is the $(1,1)$-knot K_ψ with:

$$\psi = \prod_{j=0}^{h-1} (\tau_l^{-1} \tau_m^{\varepsilon_{h-j}}) t_\beta t_\alpha t_\beta, \tag{1}$$

where[1] $\varepsilon_{h-j} = \lfloor (j+1)k/h \rfloor - \lfloor (j+2)k/h \rfloor$. Since $k < h$, we have $\varepsilon_{h-j} \in \{-1, 0\}$, for all j.

In order to find the parameters a, b, c, r for $\mathbf{t}(k,h)$, it is enough to illustrate how the Heegaard diagram $D(0,0,0,1,0,0)$ is modified by the initial application of $t_\beta t_\alpha t_\beta$ and by the successive applications of the elements τ_l^{-1} and $\tau_l^{-1}\tau_m^{-1}$ composing ψ, according to (1). In this way we construct a Heegaard diagram $D(a,b,c,1,r,0)$ representing $\mathbf{t}(k,h)$.

Actually, during the process, the Heegaard diagrams involved at each step are diagrams which can be obtained by performing a certain num-

[1] $\lfloor x \rfloor$ denotes the integral part of x.

ber $z' \in \mathbb{Z}$ of Dehn twists along the curve γ to a standard Dunwoody diagram $D(a', b', c', 1, r', 0)$ (see Figure 12). We will call this diagram $D_{z'}(a', b', c', 1, r', 0)$. These types of diagrams are depicted in Figure 12, where an arc labelled k denotes k parallel arcs. Obviously, $D_0(a', b', c', 1, r', 0) = D(a', b', c', 1, r', 0)$.

Observe that, at the end of the process, we can reduce z' to zero, since $K_{t_\gamma \psi}$ and K_ψ are equivalent knots.

Proposition 5. *Let $\mathbf{t}(k, h) \subset \mathbf{S}^3$ be a torus knot and ψ be its representation described in (1). Then $\mathbf{t}(k, h) = K(a, b, c, r)$ where $(a, b, c, r) = (a_h, b_h, c_h, r_h)$ is the final step of the following algorithm, applied for $i = h - j = 1, \dots, h$:*

- $(a_0, b_0, c_0, r_0) = (0, 0, 1, 0)$ *and* $z_0 = 0$*;*
- *for* $i = 1, \dots, h$*:*

$$\begin{cases} a_i = a_{i-1} + v \\ b_i = r_{i-1} - 2w - ud \\ c_i = d - b_i \\ r_i = a_{i-1} + v + w \\ z_i = u - \varepsilon_i \end{cases}$$

where:

$$w = \begin{cases} a_{i-1} + b_{i-1} + c_{i-1} & \text{if } z_{i-1} < -1 - \varepsilon_i \\ a_{i-1} + c_{i-1} & \text{if } z_{i-1} = -1 - \varepsilon_i \\ a_{i-1} & \text{if } z_{i-1} > -1 - \varepsilon_i \end{cases},$$

$$v = \begin{cases} -(b_{i-1} + c_{i-1})(z_{i-1} + 1 + \varepsilon_i) - b_{i-1} & \text{if } z_{i-1} < -1 - \varepsilon_i \\ 0 & \text{if } z_{i-1} = -1 - \varepsilon_i \\ (b_{i-1} + c_{i-1})(z_{i-1} + 1 + \varepsilon_i) - c_{i-1} & \text{if } z_{i-1} > -1 - \varepsilon_i \end{cases},$$

and $u = \lfloor (r_{i-1} - 2w)/d \rfloor$, *with* $d = 2a_{i-1} + b_{i-1} + c_{i-1}$.

The proof of Proposition 5 will be given at the end of this section. Now we give some examples and applications.

Remark 6. Given an admissible Dunwoody diagram $D(a, b, c, 1, r, 0)$, with $a+b+c > 0$, we fix an orientation on the arcs of $\mathcal{E}$ that induces an orientation on the corresponding curve of the Heegaard diagram in such a way that the vertex on C' labelled 1 is the first endpoint of the corresponding edge. Let $p_{a,b,c,r}$ be the number of arcs of $\mathcal{B}$ oriented from C' to C'' minus the number

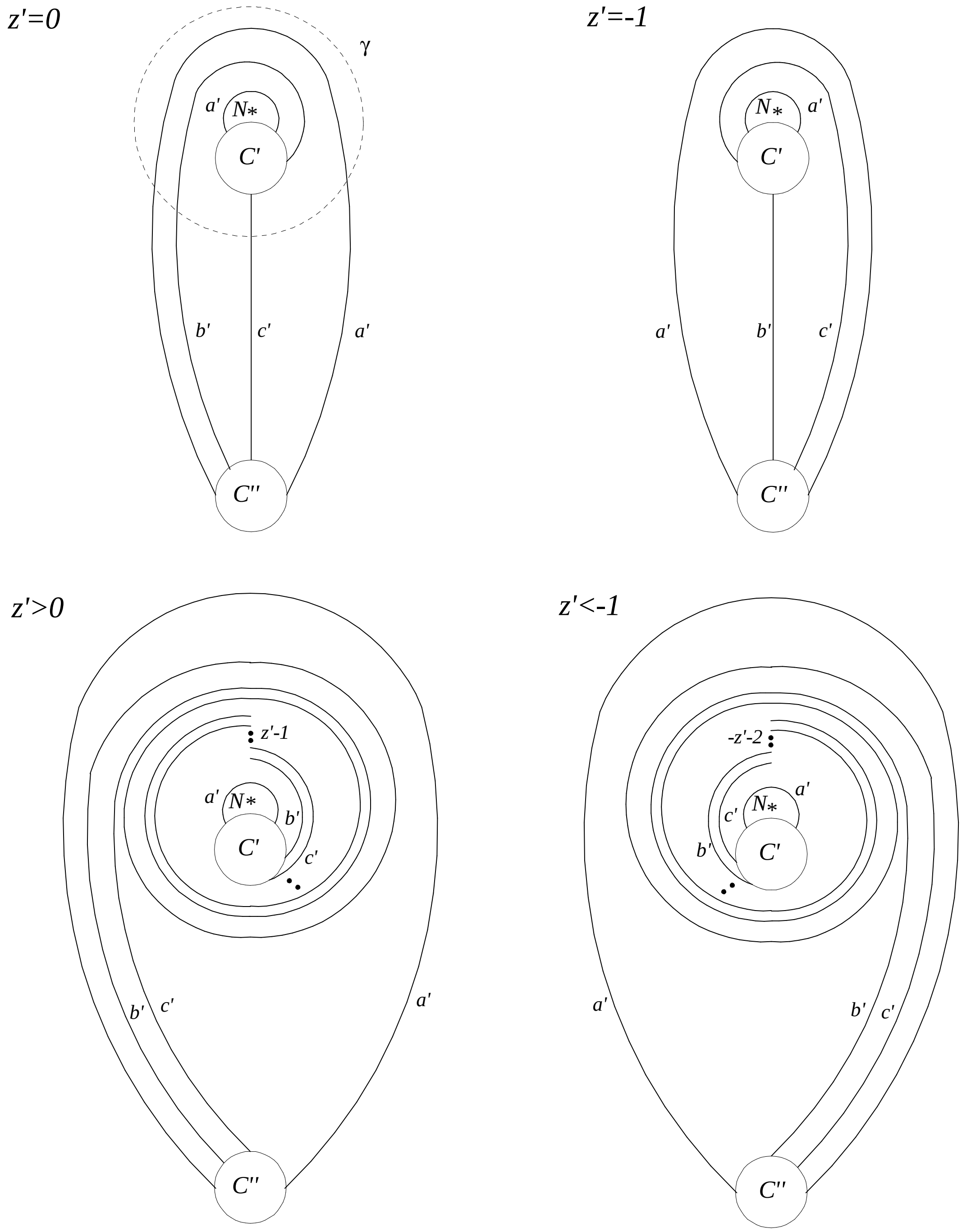

Figure 12: The Heegaard diagram $D_{z'}(a', b', c', 1, r', 0)$.

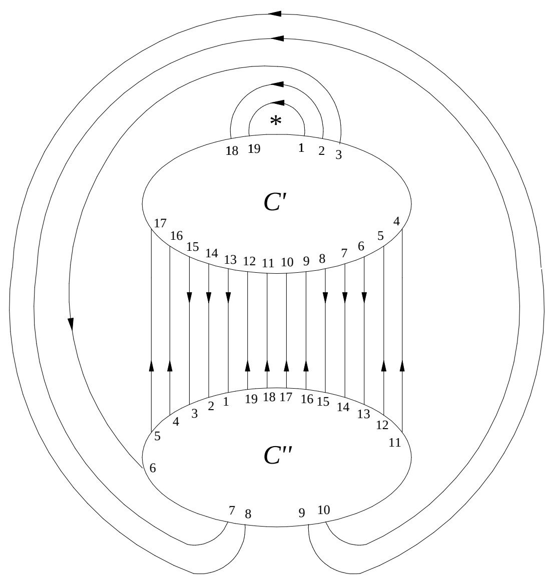

Figure 13: $D(2, 1, 14, 1, 11, 0)$.

of arcs oriented from C'' to C', and let $q_{a,b,c,r}$ be the number of arcs of $\mathcal{E}$ oriented from right to left minus the number of arcs oriented from left to right (see [7, p. 385]). If $K(a, b, c, r)$ is a $(1, 1)$-knot in $\mathbf{S}^3$, then the n-fold cyclic branched covering of $K(a, b, c, r)$ is the Dunwoody manifold $M(a, b, c, r, n, s)$, where $s = -p_{a,b,c,r}q_{a,b,c,r}$. In fact, by Proposition 2, there exists a unique $s \pmod n$ such that $M(a, b, c, n, r, s)$ is the n-fold cyclic covering of $M(a, b, c, 1, r, 0) \cong \mathbf{S}^3$, branched over $K(a, b, c, r)$. Moreover, by [7], s must satisfy the condition $q_{a,b,c,r} + sp_{a,b,c,r} \equiv 0 \pmod n$ and we have $p_{a,b,c,r} = \pm 1$.

Example. Let us consider $\mathbf{t}(5, 8)$. By (1), a representation of $\mathbf{t}(5, 8)$ is given by $\psi = \tau_l^{-1}\tau_m^{-1}\tau_l^{-1}(\tau_l^{-1}(\tau_m^{-1}\tau_l^{-1})^2)^2 t_\beta t_\alpha t_\beta$. Then, by Proposition 5, we have $\mathbf{t}(5, 8) = K(2, 1, 14, 11)$. Moreover, from the diagram $D(2, 1, 14, 1, 11, 0)$ depicted in Figure 13, we get $p_{2,1,14,11} = -1$ and $q_{2,1,14,11} = 5$. So, by Remark 6, the n-fold cyclic branched covering of $\mathbf{t}(5, 8)$ is the Dunwoody manifold $M(2, 1, 14, n, 11, 5)$, for all $n > 1$.

As an application, we explicitly determine the parametrization of $\mathbf{t}(k, ck + 1)$ as well as the Dunwoody representation of its cyclic branched coverings.

Corollary 7. *For every $c > 0$ and $k > 1$, the torus knot $\mathbf{t}(k, ck+1)$ is $K(1, k-2, 2kc-2c-k+1, k)$. Moreover, the n-fold cyclic branched covering of $\mathbf{t}(k, ck+1)$ is the Dunwoody manifold $M(1, k-2, 2kc-2c-k+1, n, k, k)$, for all $n > 1$.*

Proof. By (1), $\mathbf{t}(k, ck+1)$ is represented by $\psi = (\tau_l^{-c}\tau_m^{-1})^k\tau_l^{-1}t_\beta t_\alpha t_\beta$. Applying Proposition 5 and Remark 6 we get the statement. □

Observe that Corollary 7 agrees with the result obtained in [1] with different techniques.

Proof of Proposition 5. As shown in Figure 14, the application of $t_\beta t_\alpha t_\beta$ to $D(0,0,0,1,0,0)$ gives the diagram $D(0,0,1,1,0,0)$.

In order to simplify the notations in the figures, we set $(a_{i-1}, b_{i-1}, c_{i-1}, r_{i-1}) = (a', b', c', r')$ and $z_{i-1} = z'$. To obtain the parameters a, b, c and r, we consider the application of $\tau_l^{-1}\tau_m^{\varepsilon_i}$ to $D_{z'}(a', b', c', 1, r', 0)$.

Let us first consider the case $\varepsilon_i = 0$. We recall that the effect of τ_l^{-1} is to slide N along the longitude of the torus, illustrated by the dashed line in Figure 11, in the opposite direction to the arrow. This curve will always be represented on a Heegaard diagram by a dashed arc connecting an internal point of the arc on C', with endpoints labelled d and 1 (according to the orientation), with the corresponding point on C''. The number of intersections of the longitude with the arcs of a given diagram depends on r'. Let w be the value of r' such that the number of these intersections is minimal. Then, as illustrated in Figure 15, we have:

$$w = \begin{cases} a' + b' + c' & \text{if } z' < -1 \\ a' + c' & \text{if } z' = -1 \\ a' & \text{if } z' > -1 \end{cases}.$$

In this figure, and in the following ones, an arc labelled f denotes f parallel arcs, and we take the convention that a label of a vertex is the label corresponding to the endpoint of the first of the f parallel arcs.

First of all, we consider the case $r' = w$. In this case the longitude has $a'+v$ intersections, and the action of τ_l^{-1} is illustrated in Figure 16. We obtain $(a_i, b_i, c_i, r_i) = (a'+v, d-w, w, a'+v+w)$ and $z_i = -1$, which is the same result of the statement when $r' = w \neq 0$ (in this case $-d \leq r'-2w = -w < 0$ and so $u = -1$). If $r' = w = 0$, we have $u = 0$, and therefore the statement

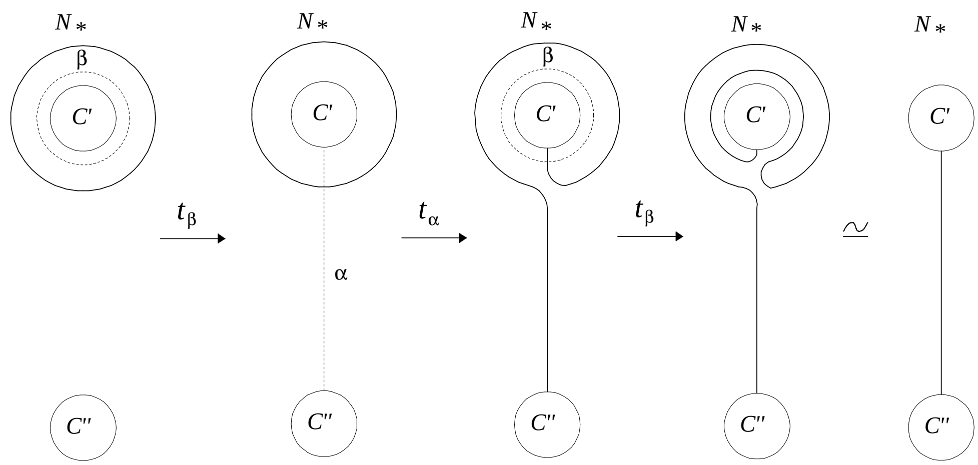

Figure 14: Action of $t_\beta t_\alpha t_\beta$ on $D(0,0,0,1,0,0)$.

gives $(a_i, b_i, c_i, r_i) = (a' + v, 0, d, a' + v)$ and $z_i = 0$; but it is easy to check that $D_0(a' + v, 0, d, 1, a' + v, 0) = D_{-1}(a' + v, d, 0, 1, a' + v, 0)$.

When $r' > w$ or $r' < w$, the result of the application of τ_l^{-1} is depicted in Figure 17. In both cases, the further $|r' - w|$ intersections determine $|r' - w|$ trivial arcs on C''. The j-th of these arcs has endpoints on C'' labelled $a' + v + d + j$ and $a' + v + d + 2(r' - w) - j + 1$ if $w < r'$, and labelled $a' + v + j$ and $a' + v + 2(w - r') - j + 1$ if $w > r'$. Each time we eliminate a trivial arc e, we glue together the two arcs whose endpoints on C' have the same label as the endpoints of e on C''. In Figure 17, the black points indicate which arcs are glued together. After the elimination of all the trivial arcs, we obtain, as above, $a_i = a' + v$ and $r_i = a' + v + w$, while the value of the other three parameters depends on the quotient of the division of $|r' - 2w|$ by d. Suppose that $r' > w$, then we have two cases:

(1) if $r' - w < w$, we obtain $b_i = d - w + r' - w = d + r' - 2w$, $c_i = w - (r' - w) = 2w - r'$ and $z_i = -1$;

(2) if $r' - w \geq w$, after the elimination of the first w trivial arcs, we obtain the diagram depicted in Figure 18. During the elimination of the remaining $r' - 2w$ arcs, each time we eliminate d arcs the parameter z' increases by one. Therefore, if u is the integer defined by $u = \lfloor (r' - 2w)/d \rfloor$, we have $b_i = r' - 2w - ud$, $c_i = (u+1)d - (r' - 2w)$ and $z_i = u$.

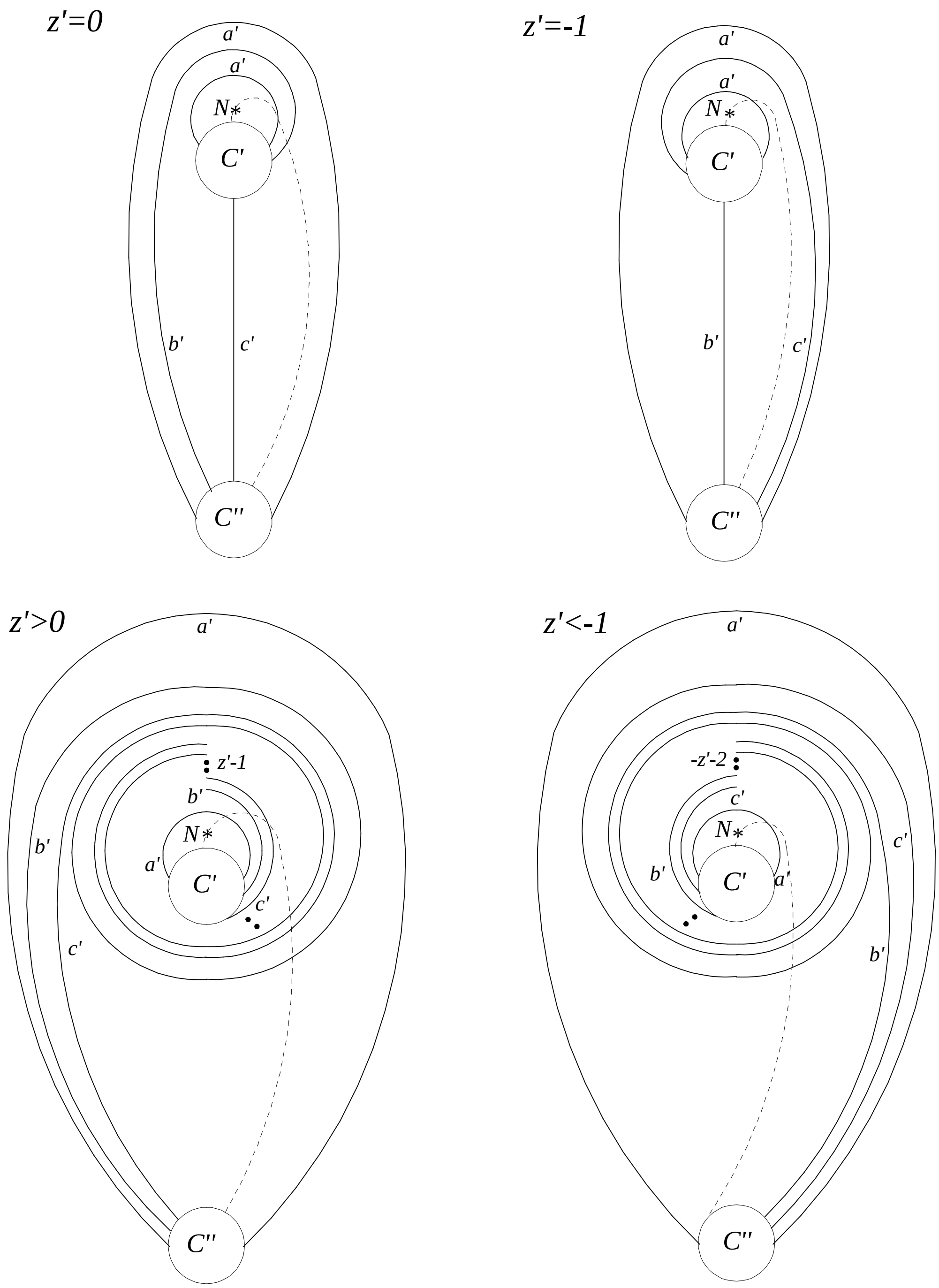

Figure 15: The parameter w.

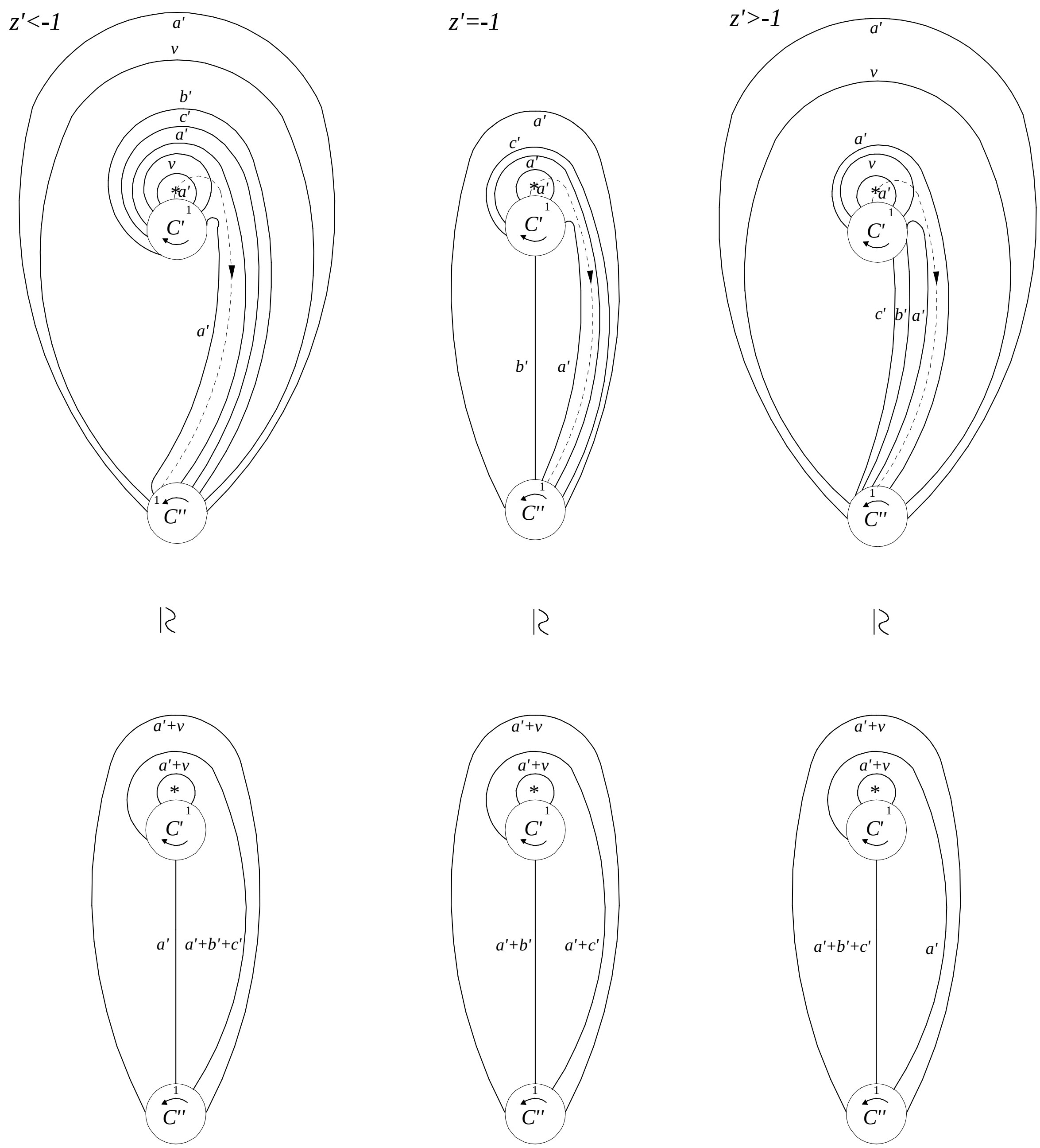

Figure 16: Action of τ_l^{-1} on $D_{z'}(a', b', c', 1, r', 0)$ for $r' = w$.

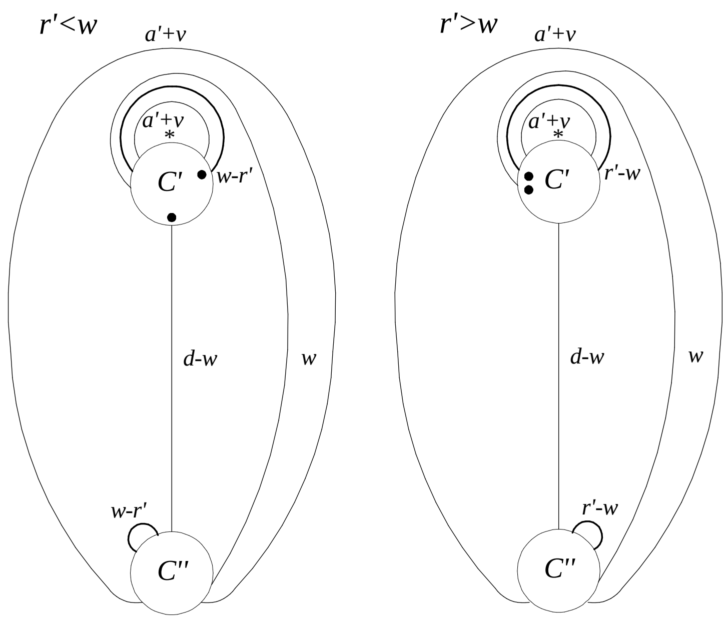

Figure 17: Action of τ_l^{-1} on $D_{z'}(a', b', c', 1, r', 0)$ for $r' < w$ and $r' > w$.

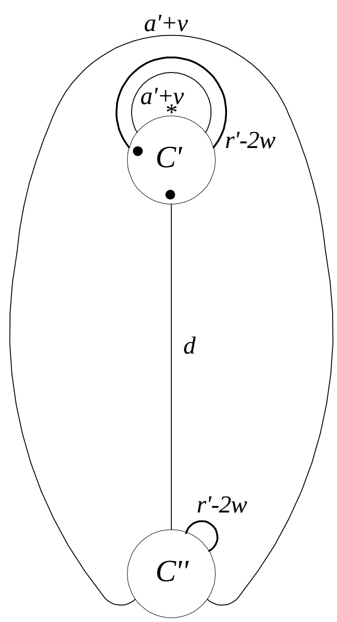

Figure 18: Action of τ_l^{-1} in the case $r' - w \geq w$.

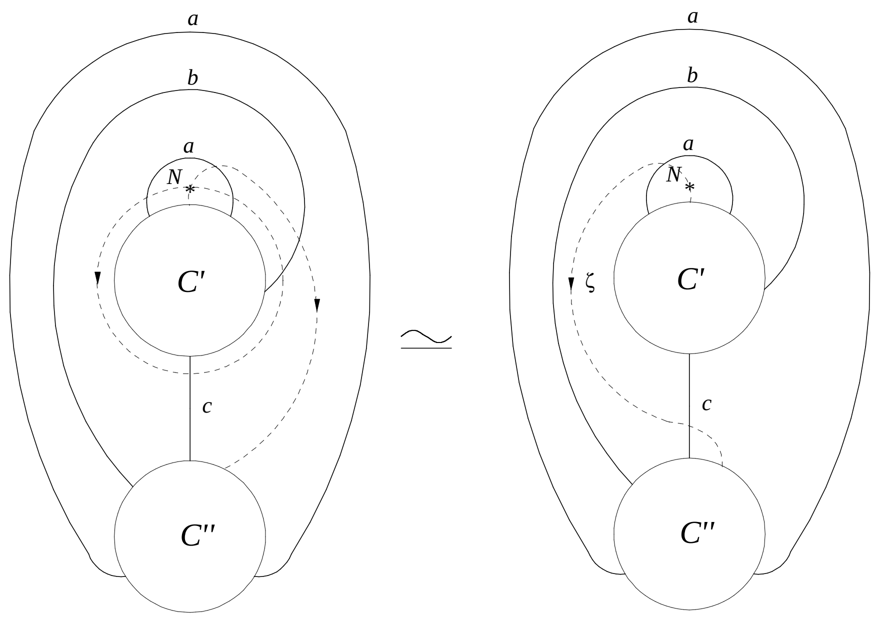

Figure 19: Action of $\tau_l^{-1}\tau_m^{-1}$.

Analysing the case $r' < w$ in an analogous way, we complete the case $\varepsilon_i = 0$.

In the case $\varepsilon_i = -1$ we examine the action of $\tau_l^{-1}\tau_m^{-1}$. This can be done in a similar way as before, since, as depicted in Figure 19, the action of $\tau_l^{-1}\tau_m^{-1}$ is equivalent to an action that moves N along the longitude ζ. $\square$

Acknowledgements

Work performed under the auspices of the G.N.S.A.G.A. of I.N.d.A.M. (Italy) and the University of Bologna, funds for selected research topics.

References

[1] H. Aydin, I. Gultekin and M. Mulazzani. Torus knots and Dunwoody manifolds. *Siberian Math. J.* **45** (2004), 1-6.

[2] G. Burde and H. Zieschang. *Knots.* De Gruyter Stud. Math. no. 5 (de Gruyter, 1985).

[3] A. Cattabriga and M. Mulazzani. Strongly-cyclic branched coverings of (1,1)-knots and cyclic presentations of groups. *Math. Proc. Cambridge Philos. Soc.* **135** (2003), 137-146.

[4] A. Cattabriga and M. Mulazzani. (1,1)-knots via the mapping class group of the twice punctured torus. *Adv. Geom.* (2004), to appear, arXiv:math.GT/0205138.

[5] D. H. Choi and K. H. Ko. Parametrizations of 1-bridge torus knots. *J. Knot Theory Ramifications* **12** (2003), 463-491.

[6] M. J. Dunwoody. Cyclic presentations and 3-manifolds. In: *Groups-Korea '94. Procedings of the International Conference* (de Gruyter, 1995), 47-55.

[7] L. Grasselli and M. Mulazzani. Genus one 1-bridge knots and Dunwoody manifolds. *Forum Math.* **13** (2001), 379-397.

[8] D. L. Johnson. *Topics in the theory of group presentations.* London Math. Soc. Lecture Note Ser. no. 42 (Cambridge Univ. Press, 1980).

[9] A. Kawauchi. *A Survey of Knot Theory* (Birkhäuser, 1996).

[10] M. Mulazzani. Cyclic presentation of groups and cyclic branched coverings of $(1,1)$-knots. *Bull. Korean Math. Soc.* **40** (2003), 101-108.

[11] J. Singer. Three-dimensional manifolds and their Heegaard diagrams. *Trans. Amer. Math. Soc.* **35** (1933), 88-111.

ALESSIA CATTABRIGA, Department of Mathematics, University of Bologna, Italy. E-mail: cattabri@dm.unibo.it

MICHELE MULAZZANI, Department of Mathematics and C.I.R.A.M., University of Bologna, Italy. E-mail: mulazza@dm.unibo.it